International Journal of Pharmaceutics 423 (2012) 93–101

Contents lists available at ScienceDirect

International Journal of Pharmaceutics

journal homepage: www.elsevier.com/locate/ijpharm

Development and characterization of immuno-nanocarriers targeting the cancer stem cell marker AC133

E. Bourseau-Guilmain[a,b], J. Béjaud[a,b], A. Griveau[a,b], N. Lautram[a,b], F. Hindré[a,b], M. Weyland[a,b], J.P. Benoit[a,b], E. Garcion[a,b,*]

[a] INSERM, U646, F-49933 Angers, France
[b] LUNAM Université, Ingénierie de la Vectorisation Particulaire, F-49933 Angers, France

ARTICLE INFO

Article history:
Received 22 February 2011
Received in revised form 30 May 2011
Accepted 1 June 2011
Available online 12 June 2011

Keywords:
Nanoparticles
CD133
Specific targeting
Antibody
Lipid nanocapsules
Caco-2
Targeted therapies
Stem cells

ABSTRACT

In the context of targeted therapy, we addressed the possibility of developing a drug delivery nanocarrier capable to specifically reach cancer cells that express the most prominent marker associated with cancer stem cell (CSC) phenotype, AC133. For this purpose, 100 nm lipid nanocapsules (LNCs) were functionalized with a monoclonal antibody (mAb) directed against AC133 according to two distinct methods: firstly, post-insertion within 100 nm LNCs of a lipid poly(ethylene glycol) functionalized with reactive-sulfhydryl maleimide groups (DSPE-PEG_{2000}-maleimide) followed by thiolated mAb coupling, and, secondly, creation of a thiolated lipo-immunoglobulin between DSPE-PEG_{2000}-maleimide and AC133, then post-inserted within LNCs. Due to the reduced number of purification steps, lower amounts of DSPE-PEG_{2000}-maleimide that were necessary as well as lower number of free maleimide functions present onto the surface of immuno-LNC, the second method was found to be more appropriate. Thus, 126 nm AC133-LNC with a zeta potential of −22 mV while keeping a narrow distribution were developed. Use of the IgG1κ isotype control-immunoglobulins produced similar control IgG1-LNCs. Micro-Bradford colorimetric assay indicated a fixation of about 40 immunoglobulins per LNC. Use of human Caco-2 cells that constitutively express AC133 (Caco-2-AC133^{high}) allowed addressing the behavior of the newly functionalized immuno-LNCs. siRNA knockown strategy permitted to obtain Caco-2-AC133^{low} for comparison. Immunofluorescence-combined flow cytometry analysis demonstrated that the epitope-recognition function of AC133 antibody was preserved when present on immuno-LNCs. Although grafting of immunoglobulins onto the surface of LNCs repressed their internalization within Caco-2 cells as evaluated by flow cytometry, AC133-specific cellular binding was obtained with AC133-LNC as assessed by computer-assisted fluorescence microscopy. In conclusion, interest of AC133-LNCs as niche carriers is discussed toward the development of CSC targeted chemo- or radio-nanomedicines.

© 2011 Elsevier B.V. All rights reserved.

1. Introduction

The cancer stem cell (CSC) model propose that cancer initiating cells capable to self-renew *ad infinitum* and to divide asymmetrically, thus expressing markers of differentiation, would be responsible of an evolutionary hierarchy among tumor cells (Visvader and Lindeman, 2008). Consequently, ongoing therapeutic strategies would preferentially target rapid dividing committed tumor cells that contribute to the tumor mass while neglecting rare slowly dividing CSCs capable to generate resistant clones. Therefore, the recognized and characterized CSC gives further hope to tumor treatment.

Among intrinsic indicators that are susceptible to tag CSCs, AC133, a glycosylation-associated epitope of the pentaspan protein CD133/prominin-1, is the best documented (Corbeil et al., 1998; Miraglia et al., 1997). Thus, AC133 monoclonal antibody-based flow cytometry and magnetic cell sorting allowed the enrichment and isolation of CSCs from a large panel of tumor types that includes blood, brain, skin, prostate, lung, breast, liver and colon cancers (Ferrandina et al., 2009; Wu and Wu, 2009). Although the role of CD133 is largely unknown and remains to be elucidated, AC133 has been linked to aggressive phenotype and associated with poor clinical outcome, notably in gliomas (Zeppernick et al., 2008) and colorectal cancers (Horst et al., 2009). In addition, *in vitro* and *in vivo* studies established that AC133-positive CSC populations survive remarkably to beam radiation (Bao et al., 2006) and are particularly resistant to chemotherapy (Angelastro and Lame,

* Corresponding author at: Institut National de la Santé et de la Recherche Médicale, Inserm U646, IBS – CHU Angers, 4 rue Larrey, 49933 Angers cedex 9, France. Tel.: +33 2 44 68 85 43; fax: +33 2 44 68 85 46.
E-mail address: emmanuel.garcion@univ-angers.fr (E. Garcion).

0378-5173/$ – see front matter © 2011 Elsevier B.V. All rights reserved.
doi:10.1016/j.ijpharm.2011.06.001

2010; Todaro et al., 2007). For those reasons, AC133-expressing CSCs located within the tumor bulk or, instead, hidden within the macroscopically normal tissue, represent significant targets to focus on.

The idea of targeted therapy, emerging from the concept of "magic bullet" proposed by Paul Ehrlich at the end of the 19th century (Winau et al., 2004), took all its signification from the work of Cesar Milstein and Georges Khöler in early 70s who developed the technique to produce monoclonal antibodies (mAbs) (Schrama et al., 2006). Although recognition can be obtained as well by use of various types of ligands, among which peptides or aptamers, mAbs are the most widely tested in the clinic, especially to block or neutralize specific molecular targets involved in cancer (Schrama et al., 2006). For instance, rituximab directed against CD20 is used within the context of lymphoma treatment (Schulz et al., 2007), trastuzumab (Herceptin®) against Her2/neu/ErbB2 within the context of breast cancer treatment (Morris and Carey, 2006), cetuximab/panitumumab against EGFR within the context of colorectal cancer treatment (Morrison et al., 2007) and bevacizumab (Avastin®) against VEGF within the context of glioblastoma treatment (Miletic et al., 2009). mAbs are also combined to radiopharmaceuticals for locoregional internal radiation therapy as exemplified within the context of glioblastoma treatment by use of ^{131}I-tenascin antibodies (Reardon et al., 2008) or ^{188}Re-nimotuzumab directed against the EGFR (Casaco et al., 2008). Alternatively, mAbs are conjugated to drug in order to make them capable to cross physiological barriers such as the blood-brain barrier as demonstrated for BDNF combined to a rat transferrin receptor mAbs (Pardridge et al., 1998) or for GDNF fusion protein combined to a human insulin receptor mAbs (Boado et al., 2008).

Recent advances in nanomedicines gave as well further resonance to targeted therapies (Peer et al., 2007). Anticancer drug combined to new nanocarriers could, indeed, present a better biodistribution profile with improved biological barrier crossing properties, leading to substantial clinical advantages including dose reduction, prevention of side effects and improvement of bioavailability within the targeted tumor cell (Peer et al., 2007). Moreover, nanoparticle combination to well define targeting agent including mAbs can greatly improve drug affinity and selectivity (Peer et al., 2007). In this context, lipid nanocapsules (LNCs) synthesized from FDA approved components through a phase-inversion process represent an alternative (Heurtault et al., 2002). With a size that can be adjusted from 20 to 100 nm with a narrow distribution, lipoprotein-like LNCs could indeed convey several anticancer drug within cancer cells among which paclitaxel (Garcion et al., 2006; Roger et al., 2009), etoposide (Lacoeuille et al., 2007) and radiopharmaceuticals (Allard et al., 2008). Their structure confer them specific skills such as multidrug resistance inhibition (Garcion et al., 2006; Roger et al., 2010), endo-lysosomal escape (Paillard et al., 2010) and capability to reach the mitochondria membrane (Weyland et al., 2011). In addition, by post-inserting a bifunctional polymer, the distearoylphosphatidylethanolamine-PEG$_{2000}$-maleimide (DSPE-PEG$_{2000}$-maleimide) in their shell to allow covalent coupling to protein thanks to creation of a thioether bond, LNCs can be functionalized and combined to thiolated proteins including monoclonal mAbs (Beduneau et al., 2007).

Thus, the objective of the present work was to develop a therapeutic drug delivery nanocarrier capable to recognize AC133-positive cells within tumors. Immuno-LNCs were synthesized by use of two distinct methods: firstly, post-insertion of DSPE-PEG$_{2000}$-maleimide to LNCs followed by mAb coupling, and, secondly, creation of a lipo-immunoglobulin between DSPE-PEG$_{2000}$-maleimide and AC133, then post-inserted within LNCs. The binding specificity of immuno-LNCs and their ability to be internalized within AC133-expressing cancer cells were evaluated on human colorectal adenocarcinoma Caco-2 cells.

2. Materials and methods

2.1. Cell culture

MOPC-31C (IgG1κ producing cells) (CCL-130^{TM}) and AC133.1 hybridomas (HB-12346^{TM}) were obtained from ATCC (American Type Culture Collection) and LGC (Laboratory of the Government Chemist) standard (Molsheim, France). MOPC-31C and AC133.1 hybridomas were cultured in RPMI 1640 medium (Lonza, Verviers, Belgium) and DMEM 4.5 g/L glucose (Lonza), respectively, supplemented with 10% of fetal bovine serum (FBS; Lonza) and 1% antibiotics (10 units of penicillin, 10 mg of streptomycin, 25 μg amphotericin B/mL; Sigma–Aldrich, Saint-Louis, USA). Cells were plated in uncoated flask at 2×10^4 cells/mL and maintained at 37 °C and 5% CO_2 until they reach a concentration of 10^6 cells/mL, before replating and purification of immunoglobulins from supernatants.

Human colon carcinoma Caco-2 cells, obtained from ATCC and LGC standard (HTB-37^{TM}), were cultured in DMEM (Lonza) containing 4.5 g/L glucose and L-glutamine. The medium was added with 10% of FBS (Lonza), 1% antibiotics (Sigma–Aldrich) and 1% of non-essential amino acids (Lonza). When cells reached 80% confluence, they were dissociated with 0.5% porcine trypsine and 0.2 g/mL EDTA (Lonza) and re-plated on uncoated plastic flasks at 15×10^3 cells/cm^2. Medium was renewed every two days.

2.2. Synthesis of immuno-LNCs

2.2.1. mAb purification and thiolation

Supernatant harvested from cultures of the AC133.1 and MOPC-31C hybridoma cell lines containing AC133 and IgG1k isotype control mAbs, respectively, was concentrated using Centricon centrifugal filter units (30 000 MWCO) according to manufacturer's instructions (Millipore, Billerica, USA). Immunoglobulins were then purified by passage over a high performance HiTrap Protein G HP column (GE Healthcare, Orsay, France) followed by elution in acid conditions and immediate neutralization according to the manufacturer's directions. mAbs buffer was changed by dialysis in Dulbecco's Phosphate Buffered Saline (DPBS; Cambrex, Verviers, Belgium) using overnight membrane dialysis (15 000 MWCO; Fisher bioblock scientific, Illkirch, France) and then concentrated with Microcon centrifugal filter units (30 000 MWCO; Millipore). The antibody concentration was determined by micro-Bradford colorimetric assay (PIERCE, Rockford, USA) according to manufacturer's instructions. For thiolation, mAbs in DPBS were incubated with 1 mg/mL of 2-iminothiolane (Traut's reagent, Fisher, Illkirch, France) for one hour in darkness under agitation. Traut's reagent was eliminated by purification of relational medium on Sephadex G25 gel filtration column (Sigma–Aldrich). mAbs were then re-concentrated to 2 mg/mL in DPBS by use of Microcon centrifugal filter units (30 000 MWCO). Thiolation of mAbs was confirmed trough a colorimetric sulfhydryl assay using Ellman's reagent (5,5′-dithiobis(2-nitrobenzoic acid)) (Sigma–Aldrich) as previously described (Beduneau et al., 2007; Iznaga Escobar et al., 1996). Briefly, 100 μL of 4 mg/mL Ellman's reagent were dissolved in DPBS and added to 1 mL of about 1 mg/mL thiolated mAb for 20 min incubation at room temperature. Free sulfhydryl levels were determined from the absorbance at 412 nm by referring to a cysteine standard curve.

2.2.2. Synthesis of LNCs

LNCs were synthesized as described previously (Heurtault et al., 2002) by using a phase inversion-based process that follows the formation of an oil/water microemulsion containing an oily fatty phase (triglycerides: Labrafac®), a non ionic hydrophilic surfactant (polyethylene glycol hydroxystearate: Solutol®) and a lipophilic surfactant (lecithins: Lipoïd®). Briefly, Solutol® HS15, Lipoïd®,

Labrafac®, NaCl and deionised water obtained from a Milli-Q plus® system (Millipore, Billerica, USA) were mixed and heated under magnetic stirring up to 85 °C. Three cycles of progressive heating and cooling in between 85 °C and 60 °C were then realized. They were finally followed by an irreversible shock induced by dilution with 0 °C de-ionized water added into the inversion phase zone. Afterwards, slow magnetic stirring was applied to the suspension for 5 min. For fluorescent staining of LNCs, the liposoluble fluorescent probe, Nile red (NR) (Sigma–Aldrich) was used as previously described (Garcion et al., 2006; Paillard et al., 2010).

2.2.3. Coupling mAbs to LNCs

Method 1: DSPE-PEG_{2000}-maleimide (Avanti Polar Lipids, Alabaster, USA) was added as a powder to a LNC suspension in order to obtain a 22 mM final concentration (optimized to incorporate a maximum amount of DSPE-PEG_{2000}-maleimide within the LNC shell). LNC and DSPE-PEG_{2000}-maleimide micelles were co-incubated for 2 h at 60 °C. A 1.5 cm × 40 cm Sepharose CL4-B column (Sigma–Aldrich) equilibrated with HEPES buffer (0.1 M, pH 7.4) was used to separate functionalized LNCs containing DSPE-PEG_{2000}-maleimide from micelles composed of free DSPE-PEG_{2000}-maleimide (loading volume: 1–1.5 mL, elution volume: 70 mL). Thus, 70 fractions of 1 mL each were sequentially collected. PEG concentration within fractions was determined using a colorimetric method based on the formation of a complex between PEG and iodine (Sims and Snape, 1980). Briefly, 5 μL of a KI/I_2 solution was added to 200 μL of sample diluted at 1:10 and the resulting absorbance of the medium was detected at 492 nm using a Multiskan® microplate spectrophotometer (Thermo Electron, Saint-Herblain, France). 10 mg of functionalized LNC containing DSPE-PEG_{2000}-maleimide were then incubated overnight at 4 °C under nitrogen atmosphere with 2 mg of thiolated mAbs on a rotating plate set at a low speed. Unbound biomolecules were removed by using a second sepharose CL-4B column as described above. Turbidimetric measurements at 600 nm were performed to evaluate LNC concentrations within the collected fractions. MicroBCA protein assay (Pierce) was used according to the manufacturer's instructions with DO analysis at 580 to determine corresponding mAbs concentrations. The number of mAbs per LNC was determined as described previously (Beduneau et al., 2007).

Method 2: DSPE-PEG_{2000}-maleimide was solubilized in DPBS through slight magnetic stirring for 30 min at room temperature. DSPE-PEG_{2000}-maleimide was then added to a solution of DPBS containing 2 mg of thiolated mAbs to obtain an equimolar concentration of 0.05 mM for the two reactive species (DSPE-PEG_{2000}-maleimide and thiolated mAbs) within a final volume of 400 μL. Overnight incubation was then performed at room temperature under low agitation. 10 mg of LNCs corresponding to 50 μL of initial suspension were then added to the formed "lipo-immunoglobulins" for 4 h incubation at 37 °C. To separate the functionalized LNC containing the newly formed lipo-immunoglobulins from micelles composed of free lipo-immunoglobulins, a sepharose CL4-B column was used as described above (method 1). Turbidimetric measurements at 600 nm and microBCA assays were performed to determine LNC and mAbs concentrations within the collected fractions as well as to calculate the number of mAbs per LNC.

2.3. Characterization of LNCs and immuno-LNCs

LNCs and immuno-LNCs were characterized for size, polydispersity index and charge distribution by dynamic light scattering using a Zetasizer® Nano Series DTS 1060 (Malvern Instruments S.A., Worcestershire, UK). LNCs and immuno-LNCs were diluted 1:1000 (v/v) in de-ionized water in order to ensure a convenient scattered intensity on the detector.

2.4. AC133 immunolabeling

Caco-2 cells were collected and dissociated using Versene (Lonza). They were then incubated with 5 μg/mL AC133 antibody (Miltenyi Biotech, Paris, France) or IgG1 isotype control (BD-Biosciences, Le Pont-de-Claix, France) for 1 h at 4 °C in DPBS containing 5% FBS and 0.02% sodium azide. After three washes in DPBS containing 5% FBS and 0.02% sodium azide, they were further incubated for 30 min at 4 °C in DPBS containing 5% FBS and 0.02% sodium azide with 20 μg/mL FITC-conjugated goat anti-mouse IgG F(ab′)2 fragment (Dakocytomation, Trappes, France). Following three more washes, cells were re-suspended in DPBS added with 2% formaldehyde and 0.02% sodium azide before flow cytometry analysis.

2.5. Flow cytometry

A BD FACSCalibur™ fluorescent-activated flow cytometer and the BD CellQuest™ software (BD-Biosciences) were used in order to proceed to flow cytometry acquisition. Analysis was carried out using WinMDI 2.9 software (Scripps Institute, La Jolla, CA, USA).

2.6. MTS/PMS surviving cell assay

2.3×10^5 Caco-2 cells were plated in 24-well plates in 400 μL of Caco-2 cell medium. After 24 h incubation at 37 °C/5% CO_2, they were treated with 20 μg/mL of AC133 antibody (Miltenyi Biotec) or immuno-LNCs at 1.1 mg/mL, thus corresponding to the same 20 μg/mL mAb concentration. After 1 h incubation at 37 °C, non-adherent cells were washed with DPBS and adherent surviving cell levels were evaluated with MTS/PMS assay using a celltiter 96 Aqueous non radioactive cell proliferation assay kit according to the manufacturer's instructions (Promega, Charbonnieres, France). Briefly, a MTS/PMS reagent diluted in DPBS (1:5) was added to the cells and incubated for 2 h at 37 °C. The soluble formazan generated by the live cells was proportional to the number of initially adherent live cells and the resulting absorbance was recorded at 490 nm using a Multiskan Ascent® microplate reader (Thermo Scientific, Courtaboeuf, France).

2.7. siRNA mediated knockdown of CD133

24 h after initial plating (see below, binding of immuno-LNCs), Caco-2 cells were transfected with 30 nM of duplex RNA oligonucleotides (Sigma–Aldrich, Saint-Louis, USA) using N-TER peptide (Sigma–Aldrich, Saint-Louis, USA) according to manufacturer's instructions. N-TER/siRNA complexes were incubated in Caco-2 cell medium during 48 h at 37 °C/5% CO_2. The sequence used to inhibit CD133 was as following: 5′-CCCUUAAUGAUAUACCUGAdTdT-3′; a sequence scramble was used as negative control 5′-GUCCGGAAUUACCAUGAGUdTdT-3′. Caco-2 cell medium was then replaced by serum-free medium containing 50% DMEM, 50% Ham's F12 (Biowhittaker) and N1 supplement (Sigma).

2.8. Binding of immuno-LNCs

Caco-2 cells were initially plated in eight-well Labtech chambers at 2×10^4 cells per well in 400 μL of serum containing Caco-2 cell medium. After siRNA treatment (see above), they were treated in serum-free medium with 23 μg/mL NR-LNCs or 23 μg/mL NR-immuno-LNCs, thus equivalent to 0.42 μg/mL of mAb, for 20 min at 4 °C under gentle agitation. The medium was then removed and

cells were washed three times with DPBS. Labtech chamber slides (Fisher bioblock scientific) were finally mounted under coverslips in fluorescent mounting medium (Dakocytomation) mixed with DPBS (1:1). Images were obtained from a fluorescence microscope (Axioscope® 2 optical, Carl-Zeiss, Le Pecq, France) and acquired through a Photometrics CoolSNAP ES camera equipped with a QImaging CRI Micro Color 2 RGB Liquid Crystal filter and by using the MetaVue™ imaging system (all from Roper Scientific, Evry, France). The images were then analysed using the MetaMorph® image analysis Software (Roper Scientific).

2.9. Cellular uptake of immuno-LNC

Caco-2 cells were plated in six-well plates with 2.3×10^5 cells per well in 2 mL of serum containing medium for 24 h. Caco-2 cell medium was then replaced by serum-free medium before Caco-2 cells were treated with 230 μg/mL NR-LNCs or NR-Immuno-LNCs thus corresponding to 4.2 μg/mL of mAb. After 2 h of incubation at 37 °C, cells washed 3 times with DPBS and dissociated using Versene (Lonza). To enable determination of the labeled molecule fraction that was effectively internalized within cells, extracellular fluorescence was quenched using 0.4% trypan blue (Sigma–Aldrich) as previously described (Paillard et al., 2010). Cells were re-suspended in DPBS containing 2% formaldehyde and 0.02% sodium azide before assessing LNC cellular internalization by flow cytometry.

2.10. Statistical analysis

XLSTAT 2011 Version 2011.1.01 (Addinsoft Paris, France) was used for data analysis. Statistical significance for each experiment was determined by a Dunnett's test. The tests were considered as significant with p values of less than 0.05.

3. Results and discussion

3.1. Design of immuno-LNCs

3.1.1. Thiolation of AC133 mAb and assessment of recognition integrity

In order to functionalize LNCs with mAbs, the bifunctional polymer DSPE-PEG_{2000}-maleimide was used: the distearoyl function being useful as a LNC shell anchor and maleimide as a chemically reactive group for conjugation with mAbs. As a prerequisite to obtain operational mAbs for conjugation to maleimide, thiol groups were introduced within AC133 mAb and IgG1κ isotype control immunoglobulins by using Traut's reagent. Traut's reagent reacted with primary amine (lysine and N-terminus) thus producing terminal sulfhydryl groups on mAbs. Although, the localization of primary amine on immunoglobulins was not exactly identified, a colorimetric sulfhydryl assay using Ellman's reagent permitted to assess that the thiolation was successful with an average of one to two thiols per immunoglobulin. As this reaction has already been described to cause loss of recognition activity, the capacity of recognition of thiolated versus native AC133 mAb was addressed on non-differentiated human colon cancer adenocarcinoma Caco-2 cells that constitutively over-express the AC133 epitope. Immunocytochemistry combined flow cytometry allowed establishing that Caco-2 cells were specifically recognized by both native and thiolated AC133 mAbs (Fig. 1A). Likewise, very similar deviations of geomean fluorescence intensity from matching IgG1κ control were obtained with native and thiolated AC133 mAbs (Fig. 1B). Those observations thus established that the thiolation of AC133 mAb by Traut's reagent have not affected the antigen-binding site of the antibody.

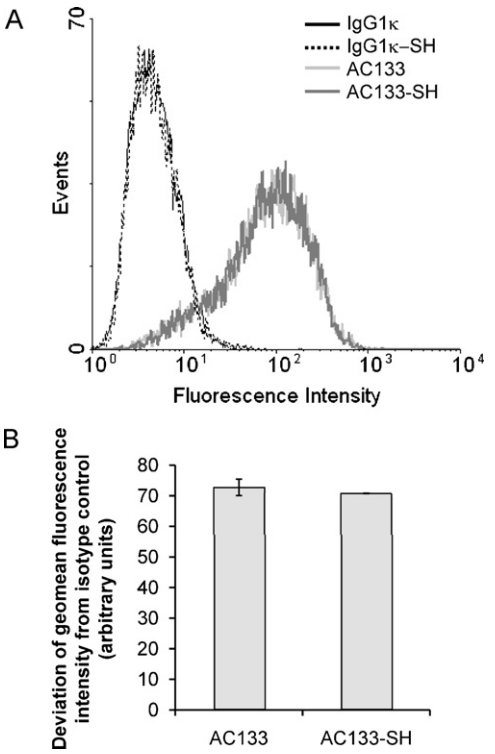

Fig. 1. mAbs thiolation does not affect the recognition site of AC133. Caco-2 cells overexpressing AC133 were incubated for 1 h at 4 °C with native and thiolated (-SH) antibodies. FITC-conjugated F(ab')2 fragments were then added to the cell suspension for 30 min at 4 °C. (A) Representative immunofluorescence combined flow cytometry analysis profiles. (B) Semi-quantitative analysis representing the deviation of geomean fluorescence intensity from isotype control obtained with native versus thiolated AC133-mAb (AC133-SH). Data represented mean ± s.e.m. of three independent experiments.

3.1.2. mAbs conjugation to LNCs and assessment of recognition activity

In order to covalently attach thiolated mAbs to LNCs, two distinct methods based on the incorporation of DSPE-PEG_{2000}-maleimide within the LNC shell were used. Firstly, as initially developed to built immunoliposomes (Huwyler et al., 1996) and utilized on LNCs for conjugation to OX26 antibody (Beduneau et al., 2007), a method of post-insertion of DSPE-PEG_{2000}-maleimide at 60 °C within LNCs followed by mAb coupling was applied (Fig. 2, method 1). Secondly, a lipo-immunoglobulin between DSPE-PEG_{2000}-maleimide and mAbs was created before being post-inserted at low temperature within the LNC shell. This last method allowed reducing the number of purification steps and the amount of DSPE-PEG_{2000}-maleimide used (Fig. 2, method 2). As immunoglobulins are proteins of about 150 kDa, the size of the LNC shell represented an important parameter to permit the coupling to an optimum number of mAbs. As such, immunoliposomes of 100 nm bearing about 30 whole antibodies were previously found optimal for targeting efficacy (Huwyler et al., 1996; Maruyama et al., 1995). Hence, conjugation of the AC133 mAbs or IgG1κ immunoglobulins was realized on native 100 nm LNCs that presented a narrow distribution and a zeta potential of about −6 mV (Table 1). Physicochemical characterization demonstrated a switch between native- and AC133-LNCs from 100 nm to 187 nm with method 1 and to 126 nm with method 2 while keeping a polydispersity index under 0.2 with both methods (Table 1). Use of the IgG1κ isotype control immunoglobulins produced similar control IgG1-LNCs (Table 1). The evolution of LNC size demonstrated the incorporation either of DSPE-PEG_{2000}-maleimide then conjugated to mAbs with method 1 or of lipo-immunoglogulins with

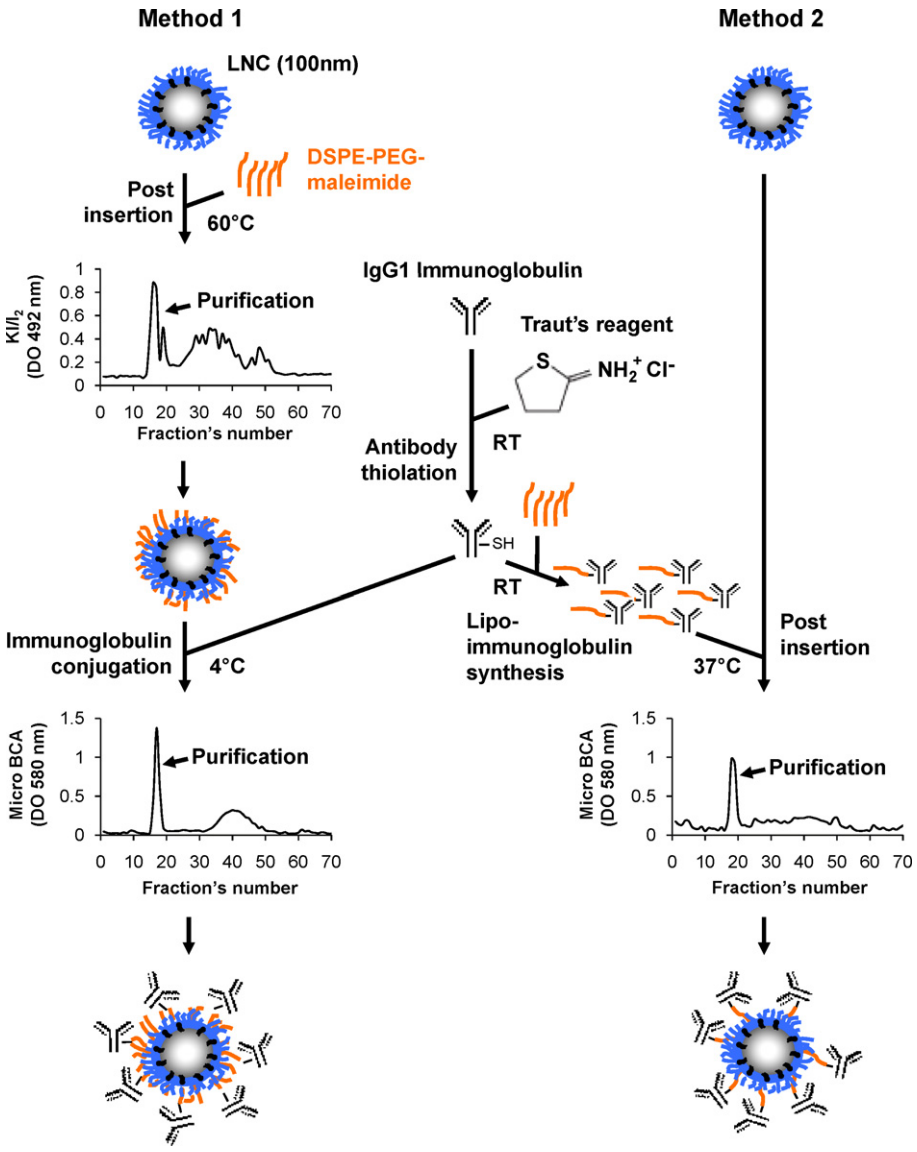

Fig. 2. Schematic representation of methods 1 and 2 for the synthesis of immuno-LNCs. Method 1 combined a first step with the insertion of DSPE-PEG_{2000}-maleimide within the LNC shell (at 60 °C) to a second step consisting in thiolated mAb conjugation to the maleimide extremity (at 4 °C). Method 2 included a first step with the creation of a lipo-immunoglobulin monomer after reaction between the thiolated mAb and the DSPE-PEG_{2000}-maleimide (at room temperature: RT) and a second step that was the post-insertion of the lipo-immunoglobulin monomer within the LNC shell (at 37 °C). Each incubation stage with LNCs was followed by a purification step onto exclusion columns as described in Section 2; arrows in front of the peak elution fractions corresponded to LNCs.

method 2. In line with this, incubation of native LNCs for 2 h at 60 °C (post-insertion parameters of method 1) or for 4 h at 37 °C (post-insertion parameters of method 2) had no impact on their initial physicochemical characteristics (size, zeta potential, polydispersity) (*cf.* Table 1). Thus, reduction in size increase of immuno-LNCs obtained with method 2 when compared with method 1 could be attributed to two parameters: (i) the amount of bifunctional polymer molecules that have been effectively incorporated (Tirosh et al., 1998) and (ii) the impact of post-insertion temperature on the conformation of incorporated bifunctional polymer that can be "brush" or "mushroom" (Tirosh et al., 1998). In spite of those evident differences, no significant variations of zeta poten-

Table 1
Characteristics of the different LNCs. PDI: polydispersity index. Note the size increase between native- and immuno-LNCs. Also the size differences between immuno-LNCs obtained with method 1 and those obtained with method 2.

	LNC	Method 1		Method 2	
		IgG1-LNC	AC133-LNC	IgG1-LNC	AC133-LNC
Size (nm)	100.1 ± 3.7	190.4 ± 7.7[#]	187.9 ± 3[#]	145.4 ± 38.4[#,*]	126 ± 10.5[#,*]
PDI	0.05 ± 0.007	0.181 ± 0.011[#]	0.179 ± 0.013 [#]	0.123 ± 0.008[#]	0.138 ± 0.040[#]
Zeta potential (mV)	−6.4 ± 3.6	−24.2 ± 0.9[#]	−24.4 ± 0.6[#]	−20.2 ± 0.6[#]	−22.8 ± 4.1[#]
mAb/LNC	–	54 ± 6	40 ± 8	28 ± 10	37 ± 13

[#] $p < 0.01$ differences from native LNCs (Dunnett's test).
[*] $p < 0.01$ differences between method 1 and 2 (Dunnett's test).

tials were found between the two methods (Table 1). Moreover, small micro-Bradford colorimetic assay associated with turbidimetric measurements established a fixation of 40 ± 8 and 37 ± 13 AC133 mAbs per LNC with method 1 and 2, respectively (Table 1). Thus, independently from the method used, immuno-LNCs displayed a conform number of immunoglobulins onto their surface to further support their functionality (Beduneau et al., 2007). However, smaller LNCs obtained when applying method 2 may be more appropriate to keep biological barrier crossing properties of the immuno-nanocarrier (Garcion et al., 2006; Paillard et al., 2010). In addition, the use of DSPE-PEG_{2000}-maleimide in large excess in method 1 (440-fold increase while leading to the same LNC antibody load as compared with method 2, *cf.* Section 2) conducted to a higher number of free maleimide functions at the surface of LNCs, already noticed with OX26 decorated-liposomes (Huwyler et al., 1996) and -LNCs (Beduneau et al., 2007). This fact could be ascribed to the steric barrier crated by LNC shell components among which is Solutol® and DSPE-PEG_{2000}-maleimide itself. The presence of free maleimide functions at the surface of LNCs may also represent the basis of undesirable side effects resulting from the interaction with free sulfhydryl functions present on natural biomolecules as exemplified by the important anti-oxidative molecule glutathione (Dringen, 2000; Friedmann, 1952).

To further validate method 2 versus method 1, recognition activity of the AC133 mAb when present on immuno-LNCs was tested on Caco-2 cells. As physicochemical characteristics of newly developed immuno-LNCs (Table 1) were found to be stable from the purification step to at least three weeks at 4 °C, immuno-LNCs were used in biological assays during this three-week period. Immunocytochemistry combined flow cytometry established that AC133 mAbs present on AC133-LNCs obtained from method 1 were capable to label Caco-2 cells with a slight increase in geomean fluorescence intensity as compared to free AC133 mAbs (Fig. 3A). Experiments developed with IgG1-LNCs demonstrated the specificity of the recognition process (Fig. 3A). The augmentation in recognition with immuno-LNCs could likely be attributed to the number of mAbs present at the surface of LNCs, thus amplifying the signal obtained from secondary antibody fixation. This is also indicative of the fact that immuno-LNCs remained stable during the staining procedure and that DSPE-PEG2000-coupling to mAb at the surface of immuno-LNCs had minor impact on the recognition integrity of thiolated AC133 mAb. Interestingly, immunocytochemistry combined flow cytometry with AC133 mAbs present on AC133-LNCs obtained from method 2 led to very similar data (Fig. 3B). Those observations demonstrated therefore the specific activity of AC133-mAbs when present on immuno-LNCs whatever the conjugation method used and conducted to use advantageous method 2 for further biological evaluation.

3.1.3. Biological properties of AC133-LNCs during incubation with Caco-2 cells

mAbs have already been used as activating- (Hicks et al., 2002) or, instead, as function blocking-immunoglobulins (Garcion et al., 2001). Although the function of the CD133 protein has not been yet elucidated, the impact of increasing concentrations (5, 10 and 20 μg/mL) of AC133 mAb versus IgG1κ control immunoglobulin was investigated on Caco-2 cell integrity (attachment and survival). Interestingly, 1-hour treatment of Caco-2 cells at 37 °C with AC133 mAb at 20 μg/mL induced a dramatic cell detachment from plastic dishes that was not observed with IgG1κ control (Fig. 4A). Caco-2 cell treatment with AC133 mAb at the dose of 5 and 10 μg/mL was not capable to trigger this effect (data not shown). Since it was previously observed that soluble and attached immunoglobulins could trigger distinct biological effects (Schwartz et al., 1991), this cell-detachment assay was used to investigate the impact of AC133 recognition on living Caco-2 cells when AC133 mAb was presented

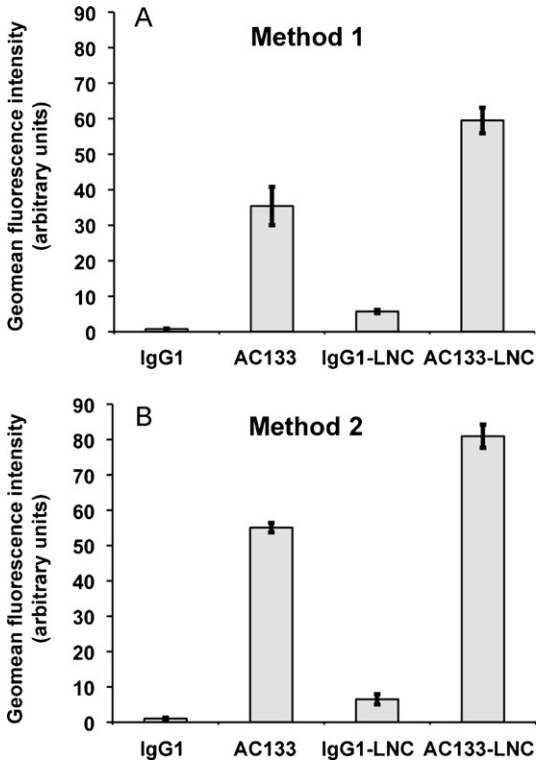

Fig. 3. AC133 coupling to LNCs does not affect its recognition site. Immunofluorescence combined flow cytometry analysis of AC133 expression was performed on AC133 expressing Caco-2 cells by using 5 μg/mL of free or LNC-bound AC133 or IgG1κ control mAbs. (A) Data obtained with mAbs conjugated to LNCs by method 1. (B) Data obtained with mAbs conjugated to LNCs by method 2. Results, expressed as mean fluorescence intensity (MFI; arbitrary units), represented mean ± s.e.m. of three independent experiments.

from AC133-LNCs. Caco-2 cells were, therefore, treated for 1-hour at 37 °C with 20 μg/mL of free mAb (AC133 versus IgG1κ isotype control) or 20 μg/mL mAb present at the surface of functionalized-LNC (thus corresponding to a 1.1 mg/mL concentration of AC133- or IgG1-LNCs). The percentage of attached living cells was then quantified by use of a MTS/PMS survival assay. Although treatment with free AC133 mAb led to 87.1 ± 0.2% detachment of Caco-2 cells from plastic dishes, treatment with AC133-LNCs did not (Fig. 4B). Those results emphasized, therefore, that AC133 mAb attached to the "LNC matrix" do not trigger similar signals as free AC133 mAb on Caco-2 cells. They also supported that immuno-LNCs do not release fully initially bound mAbs during the 1-h incubation time with AC133 expressing Caco-2 cells in the reaction medium at 37 °C, thus maintaining, at least partially, specific cell recognition capabilities.

3.2. Evaluation of AC133-specific cellular binding and uptake of AC133-LNCs

3.2.1. Binding of AC133-LNCs onto AC133 expressing Caco-2 cells

In order to plainly define the interest of AC133-LNCs to target AC133-expressing CSCs, binding of immuno-LNCs at the surface of Caco-2 cells expressing distinct levels of AC133 was investigated. siRNA-mediated knockdown of CD133 was used to down regulate AC133 expression at the surface of Caco-2 cells, thus permitting to obtain high and low AC133 expressing cells, named Caco-2-$AC133^{high}$ and Caco-2-$AC133^{low}$, respectively. Fig. 5A illustrated that use of 30 nM of siRNAs (as described in the Material and Method section) led to more than 50% reduction of AC133 expression at the surface of Caco-2 cells. Binding analysis was then performed by applying 23 μg/mL of NR-stained immuno-LNCs (carrying 0.42 μg/mL of mAbs) onto Caco-2-$AC133^{high}$ and Caco-2-

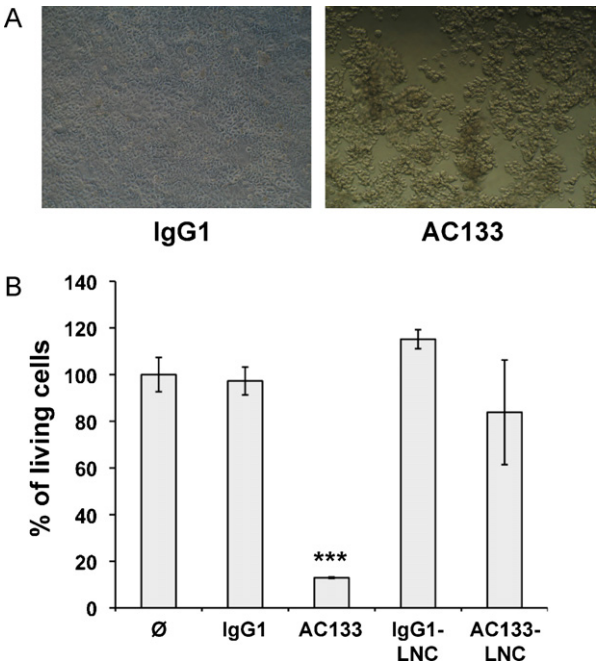

Fig. 4. Cell detachment assay corroborated the integrity immuno-LNCs during the recognition step of AC133 expressing cells. (A) Photomicrographs demonstrating that treatment of Caco-2 cell monolayers for 1 h at 37 °C with 20 μg/mL AC133 mAb triggered cell detachment while control IgG1κ immunoglobulins did not. (B) Caco-2 cells were treated for 1 h at 37 °C with IgG1κ immunoglobulins, AC133 mAb, IgG1-LNCs and AC133-LNCs at the equivalent mAb concentration of 20 μg/mL (thus corresponding to 1.1 mg/mL of LNCs). Remaining amount of attached cells was quantified by using the colorimetric MTS/PMS surviving assay. Data represented mean ± s.e.m. of three independent experiments. Dunnett's test: comparison with control untreated cells (Ø), $^{***}p < 0.001$.

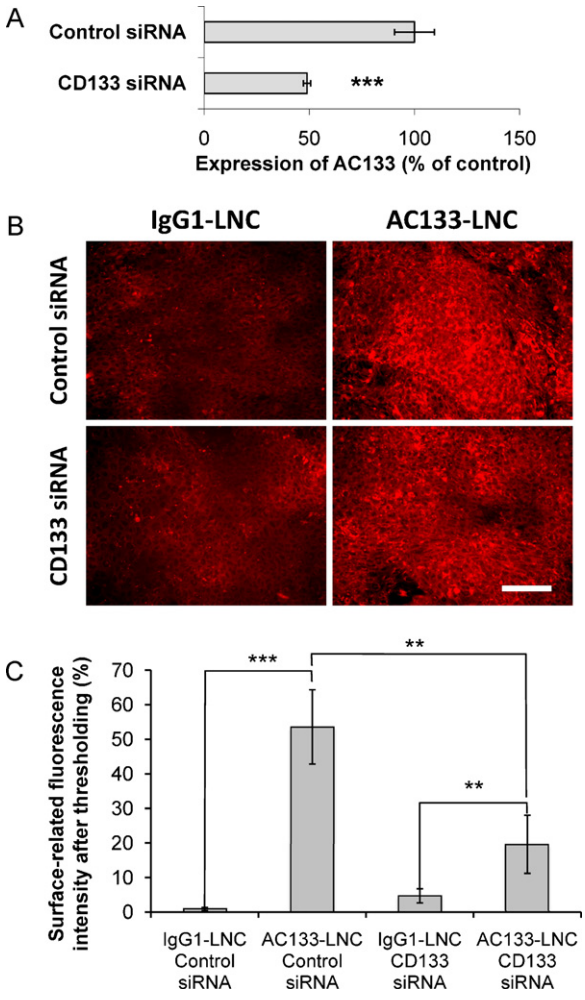

Fig. 5. AC133-dependent binding of NR-loaded AC133-LNCs onto the surface of AC133 expressing Caco-2 cells. (A) Flow cytometry analysis of AC133 expression assessing the efficiency of siRNA-mediated knockdown within Caco-2 cells. Control siRNA allowed obtaining high AC133 expressing cells (Caco-2-AC133^{high}) while CD133 siRNA allowed obtaining low AC133 expressing cells (Caco-2-AC133^{low}). (B) Fluorescent images acquired from Axioscope® 2 optical microscope of the binding of NR-loaded AC133-LNCs onto the surface of Caco-2 cells. 23 μg/mL of NR-stained immuno-LNCs (thus corresponding to 0.42 μg/mL of mAbs) were applied for 20 min at 4 °C under gentle agitation onto Caco-2 cell monolayers that have been submitted to siRNA knockdown before washing and analysis of cell surface bound fluorescence. Note that AC133-LNCs attached much better to Caco-2 cells than their IgG1κ counterparts. Note also the reduction surface bound fluorescence when expression of AC133 was reduced by use of siRNA knockdown. Bar: 50 μm. (C) Semi-quantitative evaluation of LNC binding by computer assisted fluorescence microscopy image analysis after thresholding. Results represented mean ± s.e.m. of three independent experiments. Dunnett's test: $^{**}p < 0.01$, $^{***}p < 0.001$.

AC133^{low} cell monolayers for 20 min at 4 °C under gentle agitation. LNC binding at the cell surface was evaluated by semi-quantitative computer assisted fluorescence microscopy image analysis after thresholding. As illustrated in Fig. 5B and semi-quantified in Fig. 5C, AC133-LNCs attached much better than their IgG1κ counterparts onto Caco-2 cell monolayers. In addition, reduction of AC133 expression by siRNA knockdown also led to a reduction of the binding of AC133-LNCs to Caco-2 cells (Fig. 5B and C). Importantly, whatever the situation analysed (Caco-2-AC133^{high} with control siRNA or Caco-2-AC133^{low} with CD133 siRNA) the specificity of the AC133-LNC binding was demonstrated and preserved. Those data thus established that AC133-LNCs represented a new tool to improve drug distribution and retention in the close vicinity of AC133 expressing CSCs. As such, they represented the third AC133 targeting tool and the second AC133-specific nano-object that has been so far developed with monomethyl auristatin F/AC133-mAb drug conjugates (Smith et al., 2008) and AC133-conjugated carbon nanotubes (Wang et al., 2011) both used to eliminate CSCs.

3.2.2. *Uptake of AC133-LNCs by AC133 expressing Caco-2 cells*

Having established that AC133-LNCs were capable to bind specifically to AC133-positive cells, it was further investigated whether AC133-LNCs can be internalized within Caco-2 cells. Thus, 230 μg/mL of NR-stained LNCs or immuno-LNCs (carrying 4.2 μg/mL mAbs) were incubated for 2 h at 37 °C with Caco-2 cells. After quenching of the extracellular fluorescence using trypan blue, intracellular accumulation of NR-stained LNCs was evaluated by flow cytometry. Although native LNCs were, as previously described (Garcion et al., 2006; Paillard et al., 2010; Roger et al., 2009), clearly accumulated within cells, internalization was dramatically reduced when using immuno-LNCs (Fig. 6). The inhibition of internalization of immuno-LNCs can be mainly explained by the physical characteristics of those particles, among which their size and negative zeta potential, that may have reduce their non-specific interactions with the negatively charged extracellular surface of the cell plasma membrane. As the presence of AC133 mAbs in place of IgG1κ immunoglobulins onto the surface of LNCs did not improved LNC internalization within Caco-2 cells, it can be concluded that AC133 epitope does not work as a receptor for endocytosis in contrast to LDL- (Dehouck et al., 1997; Kreuter et al., 2003) or transferrin-receptors (Olivier et al., 2002) widely used for intracellular accumulation of ApoE- or OX26-combined nanoparticles, respectively. However, a reduced cellular uptake would not necessarily preclude drug activity that is also dependent on subcellular bioavailability. As such recent data obtained with monomethyl auristatin F/AC133-mAb drug conjugates on Hep3B hepatocellular carcinoma and Kato III stomach cancer cells suggested that more

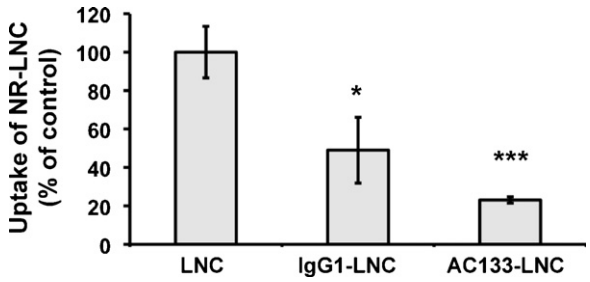

Fig. 6. Internalization of native LNCs versus immuno-LNCs within Caco-2 cells. Flow cytometry analysis revealed that treatment of Caco-2 cells for 2 h at 37 °C with either fluorescently labeled-LNCs, -IgG1-LNCs or -AC133-LNCs at 230 μg/mL (thus corresponding to 4.2 μg/mL of mAbs) led to a strongly reduced intracellular accumulation of IgG1-LNCs and AC133-LNCs as compared to native LNCs. Results represented mean ± s.e.m. of two independent experiments realized in triplicate. Dunnett's test: $^{*}p < 0.05$, $^{***}p < 0.001$.

than intracellular accumulation, routing to the lysosome may have dictated the anticancer drug activity (Smith et al., 2008). Toward the development of CSC targeted therapeutic strategies, this last data emphasized the importance of studying intracellular trafficking behavior of CSC therapeutic ligands that recognized epitopes without well-established biological functions.

4. Conclusion

In conclusion, by using the bifunctional polymer DSPE-PEG_{2000}-maleimide and synthesizing lipo-immunoglobulins further post-inserted within the LNC shell, a new nanocarrier capable to target CSCs through specific recognition of the AC133 epitope was developed. Although internalization and intracellular trafficking properties of the AC133-LNCs need further investigation, specific binding capacities onto AC133 expressing CSCs represented an interesting basis to further apply targeted therapeutic strategies notably within solid tumors. Thus, to revert CSC resistance to chemotherapy or radiotherapy, three major strategies ascribed to AC133 recognition by hydrophobic drug-loaded AC133-LNCs could be further investigated: (i) improvement of radionucleide activity-gradients exemplified by lipophilic ^{188}Rhenium complexes for induction of cell death (Allard et al., 2008), (ii) deregulation of signaling pathways normally activated, such as inhibition of sonic hedgehog pathways by cyclopamine (Bar et al., 2007), or (iii) differentiation toward a phenotype more sensitive to classical treatment by using for instance retinoic acid (Campos et al., 2010; Niu et al., 2010).

Acknowledgments

We are grateful to the Service Commun de Cytométrie d'Analyses Nucléotidiques, SCCAN, Angers, France, for skilful technical support. This work was supported by the "Institut National de la Santé et de la Recherche Médicale", the "Axe Vectorisation Tumorale" from the "Cancéropôle Grand-Ouest" and by "La Ligue Contre le Cancer" throughout an "Equipe Labellisée 2007" grant. Erika Bourseau was initially a PhD fellow from the "Conseil Général de Maine-et-Loire" and then a PhD fellow from the "Comité Départemental de Maine-et-Loire de La Ligue Contre le Cancer". Audrey Griveau was a PhD fellow from the "Conseil Général de Maine-et-Loire".

References

Allard, E., Hindre, F., Passirani, C., Lemaire, L., Lepareur, N., Noiret, N., Menei, P., Benoit, J.P., 2008. 188Re-loaded lipid nanocapsules as a promising radiopharmaceutical carrier for internal radiotherapy of malignant gliomas. Eur. J. Nucl. Med. Mol. Imaging 35, 1838–1846.

Angelastro, J.M., Lame, M.W., 2010. Overexpression of CD133 promotes drug resistance in C6 glioma cells. Mol. Cancer Res. 8, 1105–1115.

Bao, S., Wu, Q., McLendon, R.E., Hao, Y., Shi, Q., Hjelmeland, A.B., Dewhirst, M.W., Bigner, D.D., Rich, J.N., 2006. Glioma stem cells promote radioresistance by preferential activation of the DNA damage response. Nature 444, 756–760.

Bar, E.E., Chaudhry, A., Lin, A., Fan, X., Schreck, K., Matsui, W., Piccirillo, S., Vescovi, A.L., DiMeco, F., Olivi, A., et al., 2007. Cyclopamine-mediated hedgehog pathway inhibition depletes stem-like cancer cells in glioblastoma. Stem Cells 25, 2524–2533.

Beduneau, A., Saulnier, P., Hindre, F., Clavreul, A., Leroux, J.C., Benoit, J.P., 2007. Design of targeted lipid nanocapsules by conjugation of whole antibodies and antibody Fab' fragments. Biomaterials 28, 4978–4990.

Boado, R.J., Zhang, Y., Wang, Y., Pardridge, W.M., 2008. GDNF fusion protein for targeted-drug delivery across the human blood–brain barrier. Biotechnol. Bioeng. 100, 387–396.

Campos, B., Wan, F., Farhadi, M., Ernst, A., Zeppernick, F., Tagscherer, K.E., Ahmadi, R., Lohr, J., Dictus, C., Gdynia, G., et al., 2010. Differentiation therapy exerts antitumor effects on stem-like glioma cells. Clin. Cancer Res. 16, 2715–2728.

Casaco, A., Lopez, G., Garcia, I., Rodriguez, J.A., Fernandez, R., Figueredo, J., Torres, L., Perera, A., Batista, J., Leyva, R., et al., 2008. Phase I single-dose study of intracavitary-administered Nimotuzumab labeled with 188 Re in adult recurrent high-grade glioma. Cancer Biol. Ther. 7, 333–339.

Corbeil, D., Roper, K., Weigmann, A., Huttner, W.B., 1998. AC133 hematopoietic stem cell antigen: human homologue of mouse kidney prominin or distinct member of a novel protein family? Blood 91, 2625–2626.

Dehouck, B., Fenart, L., Dehouck, M.P., Pierce, A., Torpier, G., Cecchelli, R., 1997. A new function for the LDL receptor: transcytosis of LDL across the blood–brain barrier. J. Cell Biol. 138, 877–889.

Dringen, R., 2000. Metabolism and functions of glutathione in brain. Prog. Neurobiol. 62, 649–671.

Ferrandina, G., Petrillo, M., Bonanno, G., Scambia, G., 2009. Targeting CD133 antigen in cancer. Expert Opin. Ther. Targets 13, 823–837.

Friedmann, E., 1952. Spectrophotometric investigation of the interaction of glutathione with maleimide and n-ethylmaleimide. Biochim. Biophys. Acta 9, 65–75.

Garcion, E., Faissner, A., ffrench-Constant, C., 2001. Knockout mice reveal a contribution of the extracellular matrix molecule tenascin-C to neural precursor proliferation and migration. Development 128, 2485–2496.

Garcion, E., Lamprecht, A., Heurtault, B., Paillard, A., Aubert-Pouessel, A., Denizot, B., Menei, P., Benoit, J.P., 2006. A new generation of anticancer, drug-loaded, colloidal vectors reverses multidrug resistance in glioma and reduces tumor progression in rats. Mol. Cancer Ther. 5, 1710–1722.

Heurtault, B., Saulnier, P., Pech, B., Proust, J.E., Benoit, J.P., 2002. A novel phase inversion-based process for the preparation of lipid nanocarriers. Pharm. Res. 19, 875–880.

Hicks, C., Ladi, E., Lindsell, C., Hsieh, J.J., Hayward, S.D., Collazo, A., Weinmaster, G., 2002. A secreted Delta1-Fc fusion protein functions both as an activator and inhibitor of Notch1 signaling. J. Neurosci. Res. 68, 655–667.

Horst, D., Scheel, S.K., Liebmann, S., Neumann, J., Maatz, S., Kirchner, T., Jung, A., 2009. The cancer stem cell marker CD133 has high prognostic impact but unknown functional relevance for the metastasis of human colon cancer. J. Pathol. 219, 427–434.

Huwyler, J., Wu, D., Pardridge, W.M., 1996. Brain drug delivery of small molecules using immunoliposomes. Proc. Natl. Acad. Sci. U.S.A. 93, 14164–14169.

Iznaga Escobar, N., Morales, A., Nunez, G., 1996. Micromethod for quantification of SH groups generated after reduction of monoclonal antibodies. Nucl. Med. Biol. 23, 641–644.

Kreuter, J., Ramge, P., Petrov, V., Hamm, S., Gelperina, S.E., Engelhardt, B., Alyautdin, R., von Briesen, H., Begley, D.J., 2003. Direct evidence that polysorbate-80-coated poly(butylcyanoacrylate) nanoparticles deliver drugs to the CNS via specific mechanisms requiring prior binding of drug to the nanoparticles. Pharm. Res. 20, 409–416.

Lacoeuille, F., Garcion, E., Benoit, J.P., Lamprecht, A., 2007. Lipid nanocapsules for intracellular drug delivery of anticancer drugs. J. Nanosci. Nanotechnol. 7, 4612–4617.

Maruyama, K., Takizawa, T., Yuda, T., Kennel, S.J., Huang, L., Iwatsuru, M., 1995. Targetability of novel immunoliposomes modified with amphipathic poly(ethylene glycol)s conjugated at their distal terminals to monoclonal antibodies. Biochim. Biophys. Acta 1234, 74–80.

Miletic, H., Niclou, S.P., Johansson, M., Bjerkvig, R., 2009. Anti-VEGF therapies for malignant glioma: treatment effects and escape mechanisms. Expert Opin. Ther. Targets 13, 455–468.

Miraglia, S., Godfrey, W., Yin, A.H., Atkins, K., Warnke, R., Holden, J.T., Bray, R.A., Waller, E.K., Buck, D.W., 1997. A novel five-transmembrane hematopoietic stem cell antigen: isolation, characterization, and molecular cloning. Blood 90, 5013–5021.

Morris, S.R., Carey, L.A., 2006. Trastuzumab and beyond: new possibilities for the treatment of HER2-positive breast cancer. Oncology (Williston Park) 20, 1763–1771, discussion 1771–1762, 1774–1766.

Morrison, P.F., Lonser, R.R., Oldfield, E.H., 2007. Convective delivery of glial cell line-derived neurotrophic factor in the human putamen. J. Neurosurg. 107, 74–83.

Niu, C.S., Li, M.W., Ni, Y.F., Chen, J.M., Mei, J.M., Li, J., Fu, X.M., 2010. Effect of all-trans retinoic acid on the proliferation and differentiation of brain tumor stem cells. J. Exp. Clin. Cancer Res. 29, 113.

Olivier, J.C., Huertas, R., Lee, H.J., Calon, F., Pardridge, W.M., 2002. Synthesis of pegylated immunonanoparticles. Pharm. Res. 19, 1137–1143.

Paillard, A., Hindre, F., Vignes-Colombeix, C., Benoit, J.P., Garcion, E., 2010. The importance of endo-lysosomal escape with lipid nanocapsules for drug subcellular bioavailability. Biomaterials 31, 7542–7554.
Pardridge, W.M., Wu, D., Sakane, T., 1998. Combined use of carboxyl-directed protein pegylation and vector-mediated blood-brain barrier drug delivery system optimizes brain uptake of brain-derived neurotrophic factor following intravenous administration. Pharm. Res. 15, 576–582.
Peer, D., Karp, J.M., Hong, S., Farokhzad, O.C., Margalit, R., Langer, R., 2007. Nanocarriers as an emerging platform for cancer therapy. Nat. Nanotechnol. 2, 751–760.
Reardon, D.A., Zalutsky, M.R., Akabani, G., Coleman, R.E., Friedman, A.H., Herndon 2nd, J.E., McLendon, R.E., Pegram, C.N., Quinn, J.A., Rich, J.N., et al., 2008. A pilot study: 131I-antitenascin monoclonal antibody 81c6 to deliver a 44-Gy resection cavity boost. Neuro Oncol. 10, 182–189.
Roger, E., Lagarce, F., Garcion, E., Benoit, J.P., 2009. Lipid nanocarriers improve paclitaxel transport throughout human intestinal epithelial cells by using vesicle-mediated transcytosis. J. Control Release 140, 174–181.
Roger, E., Lagarce, F., Garcion, E., Benoit, J.P., 2010. Reciprocal competition between lipid nanocapsules and P-gp for paclitaxel transport across Caco-2 cells. Eur. J. Pharm. Sci. 40, 422–429.
Schrama, D., Reisfeld, R.A., Becker, J.C., 2006. Antibody targeted drugs as cancer therapeutics. Nat. Rev. Drug Discov. 5, 147–159.
Schulz, H., Bohlius, J.F., Trelle, S., Skoetz, N., Reiser, M., Kober, T., Schwarzer, G., Herold, M., Dreyling, M., Hallek, M., et al., 2007. Immunochemotherapy with rituximab and overall survival in patients with indolent or mantle cell lymphoma: a systematic review and meta-analysis. J. Natl. Cancer Inst. 99, 706–714.
Schwartz, M.A., Lechene, C., Ingber, D.E., 1991. Insoluble fibronectin activates the Na/H antiporter by clustering and immobilizing integrin alpha 5 beta 1, independent of cell shape. Proc. Natl. Acad. Sci. U.S.A. 88, 7849–7853.
Sims, G.E., Snape, T.J., 1980. A method for the estimation of polyethylene glycol in plasma protein fractions. Anal. Biochem. 107, 60–63.
Smith, L.M., Nesterova, A., Ryan, M.C., Duniho, S., Jonas, M., Anderson, M., Zabinski, R.F., Sutherland, M.K., Gerber, H.P., Van Orden, K.L., et al., 2008. CD133/prominin-1 is a potential therapeutic target for antibody-drug conjugates in hepatocellular and gastric cancers. Br. J. Cancer 99, 100–109.
Tirosh, O., Barenholz, Y., Katzhendler, J., Priev, A., 1998. Hydration of polyethylene glycol-grafted liposomes. Biophys. J. 74, 1371–1379.
Todaro, M., Alea, M.P., Di Stefano, A.B., Cammareri, P., Vermeulen, L., Iovino, F., Tripodo, C., Russo, A., Gulotta, G., Medema, J.P., et al., 2007. Colon cancer stem cells dictate tumor growth and resist cell death by production of interleukin-4. Cell Stem Cell 1, 389–402.
Visvader, J.E., Lindeman, G.J., 2008. Cancer stem cells in solid tumours: accumulating evidence and unresolved questions. Nat. Rev. Cancer 8, 755–768.
Wang, C.H., Chiou, S.H., Chou, C.P., Chen, Y.C., Huang, Y.J., Peng, C.A., 2011. Photothermolysis of glioblastoma stem-like cells targeted by carbon nanotubes conjugated with CD133 monoclonal antibody. Nanomedicine 7, 69–79.
Weyland, M., Manero, F., Paillard, A., Gree, D., Viault, G., Jarnet, D., Menei, P., Juin, P., Chourpa, I., Benoit, J.P., et al., 2011. Mitochondrial targeting by use of lipid nanocapsules loaded with SV30, an analogue of the small-molecule Bcl-2 inhibitor HA14-1. J. Control Release 151, 74–82.
Winau, F., Westphal, O., Winau, R., 2004. Paul Ehrlich – in search of the magic bullet. Microbes Infect. 6, 786–789.
Wu, Y., Wu, P.Y., 2009. CD133 as a marker for cancer stem cells: progresses and concerns. Stem Cells Dev. 18, 1127–1134.
Zeppernick, F., Ahmadi, R., Campos, B., Dictus, C., Helmke, B.M., Becker, N., Lichter, P., Unterberg, A., Radlwimmer, B., Herold-Mende, C.C., 2008. Stem cell marker CD133 affects clinical outcome in glioma patients. Clin. Cancer Res. 14, 123–129.